(33) Foti, S.; Giuoffrida, M.; Maravigna, P.; Montaudo, G. *Polym. Prepr. (Am. Chem. Soc., Div. Polym. Chem.)* **1984**, *25*, 88.
(34) Foti, S.; Montaudo, G. "Analysis of Polymer Systems"; Burk, L. S.; Allen, N. S., Eds.; Applied Science: London, 1982.
(35) Alexander, L. E. "X-Ray Diffraction Methods in Polymer Science"; Wiley-Interscience: New York, 1969.
(36) Dewar, M. J. S.; Goldberg, R. S. *J. Org. Chem.* **1970**, *35*, 2711.
(37) Johnson, J. F.; Porter, R. S.; Barrall, E. M., II, *Mol. Cryst. Liq. Cryst.* **1969**, *8*, 1.
(38) Flory, P. J. *Proc. R. Soc. London, Ser. A* **1956**, *234*, 73.
(39) Deex, O. D. Weiss, V. W. U.S. Patent 4 102 864, 1978, (Monsanto).
(40) Koningsveld, R., private communication, University of Massachusetts, 1985.

# Dynamics of Entangled Linear, Branched, and Cyclic Polymers

**Jacob Klein**

*Polymer Research,† Weizmann Institute of Science, Rehovot 76 100, Israel, and Cavendish Laboratory, Madingley Road, Cambridge, England.* *Received April 4, 1985*

ABSTRACT: We evaluate the translational diffusion coefficients and longest relaxation times for entangled linear $n$-mers, for $f$-arm star branched polymers ($n_b$-mers/arm), and for cyclic (closed ring) polymers ($n_R$-mers) in a fixed entanglement network and also in a melt of entangled linear $p$-mers. "Tube-renewal" effects for the latter case are reexamined, taking into account both hydrodynamic interactions and especially the interdependence of $p$-mer constraints about a diffusing $n$-mer; the characteristic tube-renewal time in this case becomes $\tau_{tube} \sim n^2p^{5/2}$, in contrast with earlier proposals. At very high $n$ values one expects an unscreened form for the tube-renewal time, $\tau_{tube} \sim n^{3/2}p^3$, equivalent to the "hydrodynamic sphere" diffusion of the $n$-mer in the $p$-mer melt. The diffusion coefficients and longest relaxation times for stars in a fixed entanglement lattice are calculated with a diffusion equation approach as $D_s \sim n_b^{-1} \exp(-\alpha n_b/n_c)$ and $\tau_s \sim n_b \exp(\alpha n_b/n_c)$, with $\alpha$ a constant and $n_c$ the entanglement degree of polymerization, a form similar (in the dominant exponential term) to earlier calculations. For rings the corresponding expressions are $D_R \sim \exp(-\beta n_R/n_c)$ and $\tau_R \sim \exp(\beta n_R/n_c)$, where $\beta \gtrsim \alpha$, though these are limiting forms valid for high $n_R$ ($\gtrsim 20n_c$); at lower $n_R$ values ring polymers may exhibit a quasi-linear behavior. When incorporated in melts of linear $p$-mers, the diffusion and relaxation of both stars and rings is dominated—for $n_b$ and $n_R$ greater than some crossover value of order $10n_c$—by tube-renewal effects mediated by reptation of the linear melt matrix.

## I. Introduction

The essential topological constraint on a polymer molecule in an entangled solution or melt is that it may not pass through adjacent segments. The replacement of this condition by confining the motion of any given molecule to a "tube" defined by entanglements with its neighbors has proved to be a fruitful approximation;[1,2] for the case of linear polymers the resulting translational diffusion of the molecules (and the slowest relaxation processes) takes place by reptation, and this concept forms the basis of current molecular theories of viscoelasticity.[3-6] Although viscoelastic measurements are straightforward to carry out and reasonable (but not complete) agreement with theory has been observed,[6] translational diffusion studies may provide a more direct test of the reptation approximation. Several independent approaches, including IR microdensitometry,[7] optical techniques,[8,9] NMR[10,11] methods, and neutron[12] and nuclear scattering techniques,[13,14] as well as computer simulation studies,[15] have confirmed[16] that the translational diffusion coefficient $D(n)$ of entangled linear $n$-mers varies as

$$D(n) \propto n^{-2} \tag{I.1}$$

in agreement with the reptation prediction.[2,3] Strictly speaking, eq I.1 should apply to reptation of a flexible chain in fixed surroundings or a fixed "tube"; for a non-cross-linked, entangled polymer solution or melt the tube itself is defined by intersections with the *mobile* neighbors of any enclosed molecule, so that it may, over a time $\tau_{tube}$, renew its configuration. It was argued, however,[5,17,18] that for the case of limitingly long linear molecules one would have $\tau_{tube} \gg \tau_{rep}$, the time for a molecule to renew its configuration by reptation, so that tube-renewal effects would be unimportant in entangled linear systems of sufficiently high $n$. More direct support[14,19] for the weakness of tube-renewal effects in such systems has come from diffusion studies of a linear $n$-mer in a series of chemically identical $p$-mer melts, which showed $D(n)$ to be independent of $p$ (for $p \gtrsim 3p_c$, $p_c$ being the critical length for onset of entanglements). There have also been theoretical modifications to the concept of "fixed tubes", based on the idea of constraint release as entangling molecules diffuse away.[5,17,18] These modifications do not in general change the original power-law predictions of the reptation model in the limit of high $n$ (e.g., eq I.1) in systems of linear homopolymers.

Considerably less is known, both theoretically and experimentally, for the case of entangled *nonlinear* molecules, such as star-branched or cyclic polymers. For such molecules reptation is expected to be severely suppressed,[20] and "tube renewal" may come to dominate the longest relaxation processes. For this reason, studies of the diffusion or relaxation of *nonlinear* molecules in an entangled *linear* matrix may give more direct information on tube-renewal processes than a corresponding study in a fully linear system.

A number of treatments of the diffusion and relaxation mechanisms of entangled star-branched polymers have been given. The essential idea was first presented by de Gennes,[20] who considered the motion of a symmetric $f$-arm star with $n_b$ monomers/arm, moving in a fixed lattice of noncrossable obstacles. We shall frequently find it convenient to work in terms of

$$N = n/n_c \qquad (\text{or } N_b = n_b/n_c)$$

the mean number of entanglement lengths or primitive

† Mailing address: Polymer Research Department, Weizmann Institute of Science, Rehovot 76 100, Israel.

0024-9297/86/2219-0105$01.50/0 

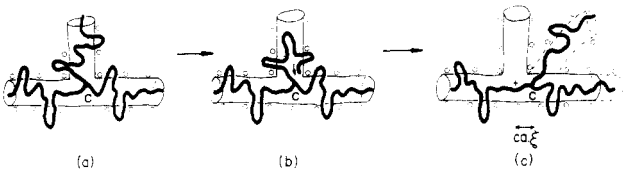


**Figure 1.** Illustration of the basic diffusion step where the center monomer C is essentially fixed over an arm-retraction process. $\xi$ is the size of the "step" from the original (+) to the new position of C: (a) starting configuration, (b) an arm has fully retracted within its original tube, and (c) can take a step into a new topological environment.

path units[3] along an entangled $n$-mer (or $n_b$-mer), where $n_c(\equiv p_c)$ is the critical degree of polymerization for entangled behavior; this is a more natural unit of length for entangled polymers, as recognized by earlier workers.[3,5]

The basic step is shown in Figure 1. Translational diffusion can only take place when an arm retracts, without crossing through any of the obstacles, as shown in Figure 1, to the position of the center monomer and then moves out again. This would move the center monomer by a lattice spacing or a tube diameter $\xi$ (equal to size of the primitive path step) in the representation of Figure 1. de Gennes[20] calculated the probability $P_1(N_b)$ of an $N_b$ arm folding back on itself as in Figure 1b as

$$P_1'(N_b) \propto \exp(-\alpha N_b) \tag{I.2}$$

with $\alpha$ a constant (where the prime indicates a temporary relation to be superseded, both for the case of $P_1$ and for other quantities), and proposed that the *rate* of such steps would be proportional to the *static* probability $P_1'$. From this he conjectured a characteristic time $\tau_{s1}'(n_b)$ for the arm relaxation

$$\tau_{s1}'(n_b) = \tau_{rep}(n_b)/P_1'(N_b) \simeq (\tau_0/n_c)n_b^3 \exp(\alpha N_b) \tag{I.3}$$

where $\tau_{rep}(n_b) = n_b^3(\tau_0/n_c)$ is the corresponding reptation time for a linear $n_b$-mer and $\tau_0$ is a microscopic jump time (independent of chain length and defined in section II). Since the center monomer moves by an independent stochastic step of size $\xi$ over the time $\tau_{s1}'$, the corresponding translational diffusion coefficient is

$$D_{s1}' \simeq \xi^2/\tau_{s1}' = (n_c\xi^2/\tau_0 n_b^3) \exp(-\alpha N_b) \simeq (D_{rep}(n_b)/N_b) \exp(-\alpha N_b) \qquad f = 3 \tag{I.4}$$

where $D_{rep}(n_b)$ is the reptation diffusion coefficient for a linear $n_b$-mer. Doi and Kuzuu[21] (using a different approach) also obtained a relation similar to eq I.3 for an arm relaxation time. Recently Graessley,[5] in a further modification of the essential idea of Figure 1, suggested

$$D_{s1}' \simeq (\xi^2/\tau_e(n_b)) \exp(-\alpha N_b) = (\xi^2/\tau_0 n_b^2) \exp(-\alpha N_b) \qquad f = 3 \tag{I.5}$$

where the characteristic time for a step $\xi$ as in Figure 1 is now taken to be $\tau_e(n_b) \simeq \tau_0 n_b^2$, the equilibration time of a linear $n_b$-mer within a tube (equivalent to its Rouse relaxation time). Pearson and Helfand,[22] using the de Gennes picture and treating the arm retraction as a dynamic process in a potential well similar to that proposed by Doi and Kuzuu, obtained a longest relaxation time for the arm of the form

$$\tau_{s1}' \propto N_b^{3/2} \exp(\alpha N_b)$$

The central assumptions of these treatment were (i) the topological environment about the star molecules was fixed (i.e., no tube-renewal effects), and (ii) the center monomer is essentially fixed over an arm relaxation time $\tau_{s1}'$.

**Table I**
**Summary of Power Exponents for Self-Diffusion and Arm-Relaxation-Time Expressions for $f = 3$**

| $D_{s1}' \propto N_b^s \exp(-\alpha N_b)$ $s$ | $\tau_{s1}' \propto N_b^t \exp(\alpha N_b)$ $t$ | ref |
|---|---|---|
| −3 | 3 | 20 |
| | 3 | 21 |
| −2 | | 5 |
| | $^3/_2$ | 22 |
| $-^5/_2$ | $^5/_2$ | 23 |
| −0.6 (±0.1) | 1.9 (±0.1) | 24 |

In a recent review, Marrucci[23] considered the case of star diffusion and relaxation where the center monomer *is* allowed to move and evaluated the star relaxation time as

$$\tau_{s1}' \propto n_b^{5/2} \exp(\alpha N_b) \tag{I.6}$$

with a diffusion coefficient

$$D_{s1}' \simeq \xi^2/\tau_{s1}' \tag{I.7}$$

Very recently Needs and Edwards[24] extended earlier work by Evans and Edwards[15] on a computer simulation of the diffusion and relaxation of a three-arm star branched polymer moving in a regular lattice of fixed noncrossable obstacles. For their translational diffusion coefficient $D_s$, they found a best fit to their data of the form

$$D_s \propto N_b^{-0.6} \exp(-B_1 N_b) \tag{I.8}$$

with $B_1$ a constant ($\simeq 0.3$) whose value was close to that calculated for their lattice.

These results, all of which have a power-exponential form in $N_b$ for both the arm relaxation time and the diffusion coefficient, are summarized in Table I.

The main *experimental* indications as to the molecular mechanism by which entangled stars relax have so far come mostly from viscoelastic data,[6,25] primarily (for the longest relaxations) the variation of zero shear rate viscosities $\eta_{os}$ with $n_b$ in star melts. In general one expects[3,5,21-23] $\eta_{os}(n_b) \propto n_b^{-1}\tau_{s1}(n_b)$, where $\tau_{s1}(n_b)$ is the overall relaxation time of one arm. A detailed review of the experimental situation will not be given here, but we note that the variation of $\eta_{os}(n_b)$ with $n_b$ is in general considerably faster than a simple power law and is indeed fitted quite well by exponential relations as in eq I.3.[22] In the present paper we consider the diffusion and relaxation mechanisms of entangled, symmetric $f$-arm star-branched molecules and of entangled ring polymers. In section II we set up our model and review reptation and tube renewal for a linear $n$-mer in a linear $p$-mer melt; in particular we reexamine the assumption of independence of tube-defining constraints and the nature of hydrodynamic interactions in the case of "tube renewal". In section III we consider mechanisms for diffusion of branched and cyclic (ring) polymers in an environment of fixed entanglements, and in section IV we extend this to the case of an environment consisting of a linear melt, where tube-renewal effects may be important. A brief account of some of these results has appeared earlier.[26,27] The case of a *melt* of stars or cyclic polymers is more subtle and is briefly discussed in the final section.

A comment is in order concerning the neglect of exact numerical coefficients and the proliferation of "approximately equal to ($\simeq$)" signs in our treatment. The question of precise preexponential factors in molecular models of polymers is challenging and is the subject of considerable ongoing effort;[28] however, the deepest insight into molecular mechanisms in polymers has often come from comparison of experiments with power-law and exponential-law—that is, relative—predictions rather than with absolute values. It is these aspects of our treatment

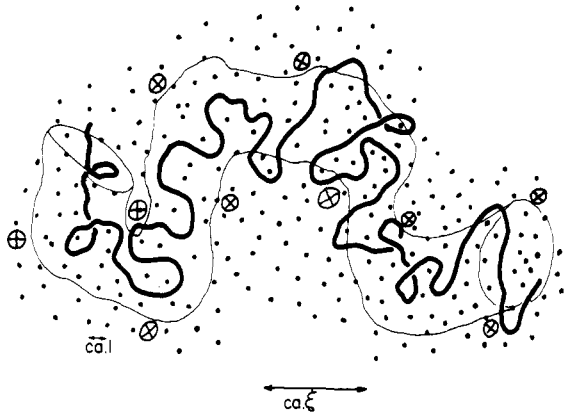


**Figure 2.** Schematic representation (not to scale) of an $n$-mer in a $p$-mer melt. The small black points are sections through the $p$-mer neighbors about the $n$-mer, separated by approximately a monomer size $l$. The tube represents the root mean square lateral freedom of the $n$-mer and has a diameter $\xi = n_c^{1/2}l$. It is represented as being defined by the locus of entanglements with "effective constraints" (open, crossed circles) a mean distance $\xi$ apart.

that we stress, and in the present discussion we shall ignore preexponential numerical factors of order $\pi$, in order not to obscure the main line of our argument; some of the more detailed calculations are relegated to Appendices.

## II. Linear $n$-mer in a $p$-mer Melt

Our model is illustrated in Figure 2. This consists of a chain with $n$ freely jointed monomers, each of size $l$, in a melt of chemically identical $p$-mers. Qualitatively we regard the "tube" about any molecule as defining the root mean square lateral freedom of motion of the molecule in the presence of its neighbors. The tube diameter $\xi$ is then the extent of this freedom and has been estimated as typically several nanometers in linear polymer melts.[29] Clearly the volume pervaded by a "tube" in this sense (for a melt) is threaded by large numbers of $p$-mer neighbors (Figure 2), whose contours are noncrossable and which provide constraints of some sort on the lateral motion. In the present model, however, we replace this picture by the usual assumption of one *effective* entanglement constraint every $n_c$ monomers along the $n$-mer, as indicated in Figure 2. The tube confining the $n$-mer may then be considered as a random walk consisting of $N = (n/n_c)$ steps (primitive path steps in the Doi–Edwards terminology). The tube "diameter" is

$$\xi = n_c^{1/2}l \tag{II.1}$$

the typical separation between the effective entanglement points, and that is also the size of a primitive step. The end-to-end distance of the $n$-mer (assuming ideality) is equal to that of the confining tube and is

$$R^2(n) = nl^2 = (n/n_c)\xi^2 = N\xi^2 \tag{II.2}$$

**Reptation.** The mobility of the linear $n$-mer in curvilinear motion within its fixed tube is $B(n) = B_0/n$ where $B_0$ is the mobility per monomer. By an Einstein fluctuation–dissipation relation, the corresponding curvilinear diffusion coefficient is given by[17]

$$D_c(n) = B(n)kT = B_0kT/n \tag{II.3}$$

The contour length of the *tube* is given by the "fully stretched" length of the primitive path

$$L_{tube}(N) = N\xi = nl/n_c^{1/2} \tag{II.4}$$

The time for the $n$-mer to diffuse curvilinearly down one tube length (the reptation or disengagement time) is then given by

$$\tau_{rep}(n) = L_{tube}^2(N)/2D_c = n^3\tau_0/n_c \tag{II.5}$$

where $\tau_0 = l^2/2B_0kT$ is a (microscopic) segmental jump time. Over a time $\tau_{rep}(n)$, the root mean square displacement of the center of mass of the $n$-mer will be $R(n)$, so that the *translational* diffusion coefficient is

$$D_{rep}(n) \simeq R^2(n)/\tau_{rep}(n) = n_cl^2/n^2\tau_0 \tag{II.6}$$

as has been experimentally confirmed in a variety of systems.[16]

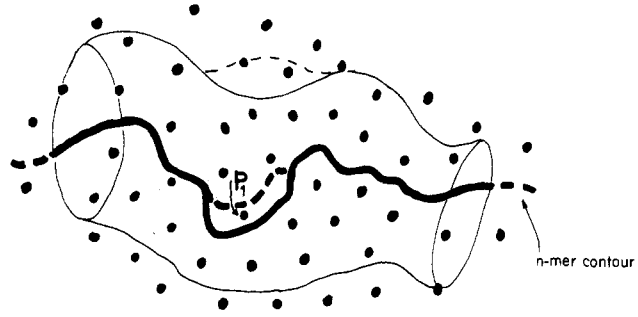


**Figure 3.** Schematic illustration of the basic tube-renewal step. A $p$-mer neighbor ($p_1$ is the section through it) of the $n$-mer chain reptates away, and a constraint on the lateral motion of the $n$ chain at the position of $p_1$ is relaxed. This may lead to a change in the mean local lateral freedom of the $n$-chain at that point, represented as a small distortion of the tube (thin broken line).

**Tube Renewal.** We briefly review the main idea:[17] the elementary step is indicated in Figure 3. Whenever any neighboring $p$-mer molecule such as $p_1$ reptates away (over a time $\tau_{rep}(p)$), a real topological change in the tube may result and the tube contour may change by a small amount. Although constraints such as $p_1$ are essentially continuous along the $n$-mer (every monomer), their overall effect is generally represented as one effective constraint (or some other small number[5]) every $n_c$-mers, and models of tube renewal have assumed that this effective constraint itself relaxes with a characteristic time comparable to $\tau_{rep}(p)$. There is no evidence that there in fact exists some unique entangling $p$-mer every $p_c$ (or $n_c$) monomers in a melt; for example, the Doi–Edwards theory,[3] which provides a detailed description of viscoelastic properties of entangled linear melts, assumes only the existence of constraints on the lateral freedom of motion of any molecule. Such constraints (the tube) need not be localized at any specific point, as for example by unique entangling molecules. We shall however continue—for convenience—to represent the tube by effective constraints that occur once every $n_c$-mers (a more detailed treatment has been given earlier[26]).

In earlier treatments the constraint relaxation time was taken as

$$\tau_c' \simeq \tau_{rep}(p) = (\tau_0/p_c)p^3 \tag{II.7}$$

with an associated characteristic local tube change equal to $\xi$, the tube diameter (or effective entanglement spacing).[40] The tube was treated as a *Rouse tube*,[30] comprising $N = n/n_c$ independent submolecules, each with the characteristic hopping time $\tau_c'$ and a longest relaxation time

$$\tau_{tube}'(N)_R \simeq N^2\tau_c' \tag{II.8}$$

taken as the time required for a tube to renew its configuration by steps as in Figure 3.[17]

The assumption of *independent* constraints is not necessarily correct, as already noted.[17,36] Let us break up the $n$-mer ($n \geq p$, say) into $n/p$ *blobs*, each with $p$ mo-

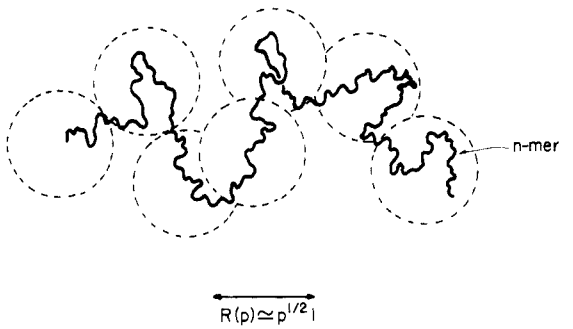


**Figure 4.** An $n$-mer in a $p$-mer melt will be in contact with segments from $p$-mer molecules whose centers are within approximately one $p$-mer radius of the $n$-mer molecule. Roughly speaking, these $p$-molecules must have their centers within "blobs" of radius $R(p) = p^{1/2}l$ centered on the $n$-mer contour.

nomers,[41] Figure 4; then the number $p_i$ of *different* $p$ molecules contributing to constraints on the $n$ molecule *within each blob* is roughly the number of $p$-mers with centers originating in the blob volume, i.e., $p_i \simeq (p^{1/2}l)^3/pl^3 = p^{1/2}$ independent molecules. Since the section of $n$-mer within a $p$ blob is itself $p$ monomers long, it will be in contact with $p$ neighboring segments such as $p_1$ (Figure 3). *But only $p_i$ of these are independent*; i.e., each of the $p_i$ $p$-mers in a blob contributes on average $p/p_i$ neighboring segments to the $n$-mer within the blob, for a total of $p$ neighboring segments in all. Each time that a $p$ molecule reptates away, $p/p_i$ neighboring segments of the $n$-mer will "disappear": the effective disappearance frequency of these neighboring constaints will thus be increased by a factor $p/p_i$, and their relaxation time $\tau_c$ will then become

$$\tau_c \simeq \frac{\tau_{rep}(p)}{p/p_i} = \frac{\tau_{rep}(p)}{p^{1/2}} \tag{II.9}$$

It is not obvious that a similar consideration must apply to the "disappearance" rate of *effective* entanglement constraints, which are taken to occur every $n_c$-mers and which make up the Rouse tube. Thus, if these indeed consisted of individual uniquely entangling $p$ molecules, there would be $p/p_c$ of them in a blob, and as long as

$$p/p_c \ll p_i \simeq p^{1/2} \tag{II.10}$$

the effective constraints *may* be assumed independent (as in earlier treatments[5,17,18,26]). The condition in (II.10) in fact holds in all practical circumstances. (It only breaks down for $p \gg p_c^2$, i.e., $p \gg 10^4$ monomers for typical values of $p_c = O(10^2)$ monomers. Such high degrees of polymerization are exceptional.) In this case the relaxation time for effective constraints remains $\sim\tau_{rep}(p)$ rather than $\tau_c$.

The other view (which we adopt here) is to regard each of the $N = n/n_c$ effective constraints on the $n$-chain as in some sense a combined effect of the $n_c$ neighboring segments on each "entanglement length" of the $n$-chain, with a mean relaxation time $\tau_c$ *equal* to that of these neighboring segments (eq II.9). It is not at present possible on experimental ground to say which view (if either) is correct; in the present treatment we shall assume an enhanced relaxation rate for the *effective* constraints given by eq II.9 rather than by eq II.7.

The corresponding "mobility" $\mu$ of each effective constraint (equivalent to the "bead mobility" in the Rouse model) is associated with the jump of size $\xi$ over the time $\tau_c$ and is given by

$$\mu = \xi^2/\tau_c kT \tag{II.11}$$

The longest relaxation time in the Rouse model now becomes

$$\tau_{tube}(N)_R \simeq N^2\tau_c = N^2\tau_{rep}(p)p^{-1/2} = (p^{5/2}/nn_c^2)\tau_{rep}(n) \tag{II.12}$$

on substituting for $\tau_c$ from (II.9), and the tube-renewal diffusion coefficient is

$$D_{tube}(N)_R \simeq R^2(n)/\tau_{tube}(N)_R = (nn_c^2/p^{5/2})D_{rep}(n) \tag{II.13}$$

From (II.13) we see that diffusion by (Rouse) tube renewal is dominant whenever $n \gg n^*$, where

$$n^* = p^{5/2}n_c^{-2} \tag{II.14}$$

In highly entangled matrices ($p \gg p_c$) the crossover value for $n$ becomes large and suggests the possibility[26] that the motion of the $n$-mer via tube-renewal steps may not be hydrodynamically screened (which is the assumption underlying the use of the Rouse model above for tube-renewal dynamics) but rather may behave in a non-free-draining or unscreened manner.[31] There are two ways of looking at this. In a purely formal sense we may depict the tube-renewal process (Figure 3) in terms of a *Zimm* model.[31] Consider now the Zimm "hydrodynamic coupling parameter" $h$ (where $h \ll 1$ or $h \gg 1$ for free-draining (screened) or non-free-draining (unscreened) behavior, respectively); in our notation, with a tube of $N$ segments each of size $\xi = n_c^{1/2}l$ and a mobility $\mu$, we have (ref 31, eq 69, ignoring numerical constants)

$$h = N^{1/2}\mu^{-1}/n_c^{1/2}l\eta(p) \tag{II.15}$$

where $\eta(p)$ is the viscosity of the $p$-mer matrix. For purely reptating $p$ molecules, the viscosity is given by[3]

$$\eta(p) \simeq E\tau_{rep}(p) \tag{II.16}$$

where $E$ is the elastic modulus of the entanglement network associated with the $p$ chains

$$E = kT/p_c l^3 \tag{II.17}$$

Inserting the expressions for $\mu$, $\eta(p)$, $\tau_c$, and $E$ (eq II.11, II.9, II.16, and II.17) into (II.15), we find

$$h = p_c^{-1}(n/p)^{1/2} \tag{II.18}$$

Thus for sufficiently large $n > n^{**}$, where

$$n^{**} = pp_c^2 \tag{II.19}$$

we expect unscreened or Zimm-like tube renewal. (We note however that for typical values of $p_c$ ($O(10^2)$) the transition to the unscreened limit occurs at $n$ values that may be unattainable in practice.)

The second approach to understanding the nature of the unscreened behavior of the $n$-mer in the tube-renewal mode involves a more basic consideration. The motion of any polymer segment, in an overlapping polymer solution under force **f**, creates a backflow velocity $\delta\mathbf{v}$ at **r**, which in the absence of screening has the form

$$\delta\mathbf{v} \sim \frac{\mathbf{f}}{\eta_0}\frac{1}{r} \tag{II.20}$$

where $\eta_0$ is the solvent viscosity. The presence of additional segments reduces the magnitude of this backflow field to a form

$$\delta v \sim (1/r)e^{-\lambda r} \tag{II.21}$$

The screened form has been considered by Edward and Freed[32] and arises because of the small monomer concentration fluctuations at the positions of the screening segments; the net result is that over dimensions much larger than the segment–segment correlation distance $1/\lambda$, the backflow field becomes negligible, and the free-draining

Rouse model is essentially applicable. Our present conjecture is that in the *melt* (over sufficiently large spatial scales) one returns to the unscreened (or non-free-draining) from (II.20) but where $\eta_0$ is now the viscosity of the *melt medium* itself (see also ref 33). In this case one expects the usual Zimm relations to hold in the limit of large $N$. It is important to note that this picture is of relevance only when it is the *tube-renewal mechanism* that determines the entangled $n$-mer dynamics, since it is then that lateral processes (Figure 3) are dominant. For the usual reptation mechanism ($N \simeq P \gg 1$) the determining motion is curvilinear, and one expects backflow effects to be small[2] (in head-on motion only a small perturbation of the medium is required for translation of the molecule).

In the limit of very large $N/P$, therefore, we may replace the free-draining, or screened, Rouse[30] values for $D_{tube}$ (eq II.13) and $\tau_{tube}$ (eq II.12) by their Zimm counterparts[31]

$$D_{tube}(N)_Z \simeq \frac{kT}{N^{1/2}\xi\eta(p)} = \frac{kT}{R(N)\eta(p)} = \frac{n^{3/2}}{p^3}p_c D_{rep}(n) \tag{II.22}$$

$$\tau_{tube}(N)_Z \simeq \frac{R^2(n)}{D_{tube}(N)_Z} = \frac{p^3}{n^{3/2}p_c}\tau_{rep}(n) \tag{II.23}$$

Daoud and de Gennes have pointed out[18] that for an $n$-mer diffusing in a given $p$-mer melt, in the limit of large $n$, the $n$-mer must behave like a hydrodynamic sphere of radius $R(n)$ moving within a continuous medium. In this case its diffusion coefficient reverts to a Stokes–Einstein form

$$D_{SE}(N) = kT/6\pi\eta(p)R(n) \tag{II.24}$$

We note that this form is essentially identical with that of the screened tube-renewal diffusion coefficient (eq II.22) applicable in the limit of large $n/p$.

To summarize: for a linear $n$-mer in a linear $p$-mer melt ($n,p \gg p_c$) we expect enhancement of the rate of release of topological constraints about the $n$-mer due to the interdependence of its $p$-mer neighbors. On the assumption that a similar enhancement applies to the rate of effective "entanglement constraint" release, a number of regimes are indicated:

(i) In homopolymers $n \simeq p$, we see from eq II.13 that self-diffusion and relaxation are dominated by reptation for all $p > p_c^{4/3}$, i.e., above a few entanglement lengths.

(ii) For $p_c \ll p \leq n^* = p^{5/2}p_c^{-2}$ (eq II.14) the behavior of the $n$ chain is dominated by reptation (with tube renewal only a minor contributing mode), and is characterized by $D_{rep}(n)$ and $\tau_{rep}(n)$ (eq II.6 and II.5).

(iii) For $n \gg n^*$, tube renewal (Rouse-like) becomes dominant, with a diffusion coefficient and longest relaxation time given by $D_{tube}(N)_R$ and $\tau_{tube}(N)_R$ (eq II.13 and II.12, respectively).

(iv) At very large $n$ values, $n > n^{**} = pp_c^2$, (eq II.19) the tube-renewal steps become effectively unscreened and the Zimm expressions $D_{tube}(N)_Z$ and $\tau_{tube}(N)_Z$ apply (eq II.22 and II.23). These have essentially the same form as the Stokes–Einstein hydrodynamic sphere limit noted by Daoud and de Gennes. Comparison of $D_{tube}(N)_R$ with $D_{tube}(N)_Z$ shows a self-consistent crossover between them at the same value of $n \simeq n^{**}$ (i.e., non-free-draining tube-renewal dynamics dominate at $n > n^{**}$).

What of the limit $p \gg n > p_c$? The number of neighboring $p$-mers in contact with the $n$-mer is of order $n$, while the number of *independent* $p$-chains is still $p_i \simeq p^{1/2}$, the number of $p$-mers in a $p$-blob. If $p^{1/2} > n$, the probability of neighbor interdependence (Figure 4) becomes low and the relaxation time of effective entangling constraints reverts to the value $\tau_c' \simeq \tau_{rep}(p)$. For linear $n$-mers this makes little difference, since for $n < p$ the behavior of the $n$-mer is in any event dominated by reptation in the essentially fixed $p$-mer surroundings. However, for nonlinear $n$ chains (stars and rings) in a linear environment, where reptation of the $n$-mer is suppressed, tube renewal may become dominant even at $n \ll p$. In the present treatment we assume that the limit $p > n^2$ is not attained and that the more rapid constraint relaxation time $\tau_c$ is applicable.

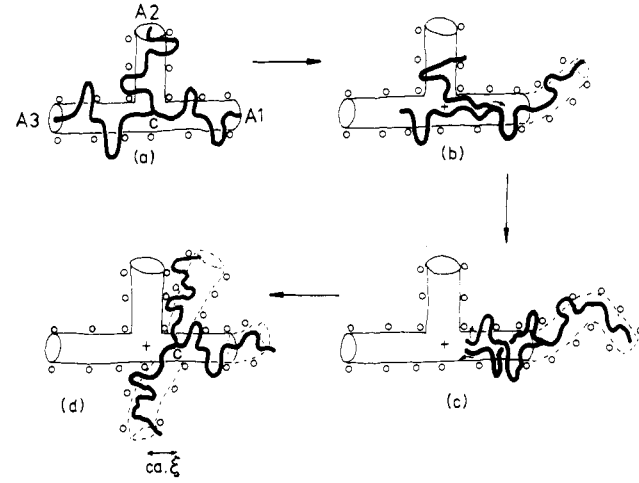


**Figure 5.** An alternative mechanism for center-of-mass diffusion. The center monomer C of a star starting with configuration (a) moves down one of the arm tubes, "dragging" the other arms with it (b) until (c) they are fully retracted past the original position of C(+). The arms can now return to new topological configurations (d), allowing C to make a diffusive step $\xi$.

## III. Diffusion of $f$-Arm Stars and of Cyclic Ring Polymers in a Fixed Obstacle Lattice

***f*-Arm Stars.** In addition to the mechanism proposed by de Gennes and described in section I (and Figure 1), there is another mode of motion by which the center monomer of an $f$-arm star may take a stochastic topological step in a fixed-obstacle field. This is illustrated in Figure 5 (where $f = 3$ for clarity) and involves motion of the center monomer C a distance $q_2$ primitive steps down one of the $f$ "tubes" emanating from the center of the star; the other $(f-1)$ arms are "dragged" behind C, as shown (Figure 5b). Whenever the ends of the $(f-1)$ arms being dragged up a given tube pass the original position of the center monomer (Figure 5c), they completely escape their original tubes, and a real stochastically independent step $\xi$ can be taken by the center monomer (Figure 5d).

We wish to evaluate the overall expectation time $\langle\tau\rangle$ for the process illustrated in Figure 5c to occur; i.e., for $q_2 \rightarrow N_b$. To do this we note that the motion of C up an arm (i.e., in an increasing $q_2$ direction) is opposed by an entropic force.[20] Qualitatively, the origin of this entropic force is easy to appreciate: suppose C moves one step up an arm; i.e., $q_2 \rightarrow q_2 + 1$. Then the "leading" branch end, (A1, Figure 5) has a choice of $z$ (say) new positions it can adopt and an entropy gain $\Delta S \simeq k \ln z$. On the other hand, the reverse step $q_2 + 1 \rightarrow q_2$ allows *each* of the ends (A2, A3, etc.) of the $(f-1)$ other branches a choice of $z$ new positions, with an entropy gain $\Delta S \simeq k(f-1) \ln z$, i.e., a net entropy gain $k(f-2) \ln z$ for a backward step (Figure 6). This implies that the motion of C in an increasing $q_2$ direction is opposed by a force whose origin is entropic and results in an effective potential field $U(q_2)$. The qualitative argument just given would result in

$$\delta U'(q_2) \simeq T\Delta S = kT(f-2) \ln z \qquad \text{(overestimate)} \tag{III.1}$$

In practice this is an overestimate, since it is possible for the center monomer to take a backward ($q_2 + 1 \rightarrow q_2$) step by a "doubling up" of segments along an arm contour without the motion of an arm end (Figure 5c).

A better estimate for $U(q_2)$ is obtained by considering the equilibrium probability $P_2(f,q_2)$ that $(f-1)$ arm segments, each $q_2$ steps in length, occupy part of a single "tube" as in Figure 5b. Now the de Gennes expression for $P_1'(q)$, eq I.2, gives the equilibrium probability that a $q$-step walk folds back on itself without enclosing obstacles or, equivalently, that two walks, each of $q/2$ steps, occupy a single tube. This leads us to expect an equilibrium probability $P_2$ for $(f-1)$ walks, each of size $q_2$, of the form

$$P_2(f,q_2) = P_1'(2q_2(f-2)) = A \exp(-2q_2(f-2)\alpha) \quad \text{(III.2)}$$

where $A$ is a normalization constant[42] independent of $q_2$. Recently the probability $P_1(N)$ that an $N$-step linear chain retraces its contour without enclosing any obstacles (on a lattice) has been recalculated[22,24] and shown to have the form

$$P_1(N) \simeq N^{-3/2} \exp(-\gamma N) \quad \text{(III.3)}$$

at large $N$, where $\gamma$ is of order unity and depends on the coordination $z$ of the lattice (we shall later identify $\gamma$ with the exponential argument $\alpha$ introduced earlier).

We now estimate $\delta U(q_2) = T\Delta S$, where $\Delta S$ is the entropy difference between the states $q_2$ and $(q_2 - 1)$, i.e.

$$\Delta S = S(P_2(f,q_2)) - S(P_2(f,q_2-1)) = k[\ln P_2(f,q_2) - \ln P_2(f,q_2-1)] \quad \text{(III.4)}$$

where $S(P) = -k \ln P$ is the configurational entropy of the conformation with entropy $P$. Using the purely exponential form of $P_2$ (eq III.2), we find

$$\delta U_{q_2 \rightarrow q_2-1} = -2\alpha(f-2)kT \quad \text{(III.5)}$$

Thus the potential $U(q_2)$ opposing the motion of the center monomer C is

$$U(q_2) = 2\alpha|q_2|(f-2)kT \quad \text{(III.6)}$$

where we have written $|q_2|$ to indicate that C can move up *any* of the $f$ arms: we note that using the power exponential form of $P_1$ (eq III.3) leads to a small (logarithmic) correction to $U(q_2)$, which becomes negligible at large $q_2$.

The problem now becomes that of diffusion of a point (i.e., the star center C) in the centrosymmetric potential field $U(q_2)$, which is governed by the standard diffusion equation of a particle in a potential field

$$\left[\frac{\partial}{\partial t} - D_2\frac{\partial}{\partial x_2}\left(\frac{\partial}{\partial x_2} + \frac{1}{kT}\frac{\partial U}{\partial x_2}\right)\right]P(x_2,t) = 0 \quad \text{(III.7)}$$

where $x_2 = q_2\xi$ is the distance corresponding to $q_2$ steps of the center monomer down a tube, $P(x_2,t)\,dx_2$ is the probability that the center monomer is between $x_2$ and $(x_2 + dx_2)$ at time $t$ (down any of the $f$ tubes), $D_2$ is the *curvilinear* diffusion coefficient of the $f$-arm star (i.e., $D_2 = kT/\zeta$, where $\zeta$ is the friction coefficient of the star in curvilinear motion), and $U(q_2) = U(x_2) = 2\alpha|x_2/\xi|kT(f-2)$ as given by eq III.6. The boundary conditions on (III.7) are

$$P(N_b\xi,t) = P(-N_b\xi,t) = 0 \quad \text{(III.8)}$$

where $N_b\xi$ is the length of an arm tube.

Whenever the center monomer C reaches the end of an arm tube (e.g., Figure 5c), a stochastic topological step of size $\xi$ may be taken; the corresponding three-dimensional diffusion coefficient $D_{s2}$ is then given by

$$D_{s2} \simeq \xi^2/\langle\tau\rangle \quad \text{(III.9)}$$

where $\langle\tau\rangle$ is the expectation time for the first passage process $q_2 \rightarrow N_b$ (Figure 5c) to occur. Equation III.7 is solved to yield this expectation time (Appendix I), and its dominant term has the form

$$\langle\tau\rangle \equiv \tau_{s2} \simeq (\tau_{rep}(n_b)/\alpha^2N_b^2)\exp[2\alpha N_b(f-2)] \quad \text{(III.10)}$$

(omitting a weak preexponential $f$ dependence), where $\tau_{rep}(n_b)$ is as before (eq II.5) the reptation time for a linear $n_b$-mer. The corresponding diffusion coefficient is then (eq III.9)

$$D_{s2} \simeq \alpha^2N_bD_{rep}(n_b)\exp[-2\alpha N_b(f-2)] \quad \text{(III.11)}$$

where $D_{rep}(n_b)$ is the reptative diffusion coefficient for a linear $n_b$-mer (eq II.6).

The form of the diffusion coefficient in eq III.11 differs considerably in the preexponential dependence on $N_b$ from the forms proposed earlier (e.g., eq I.4, I.5, and I.7 by factors $N_b$ to $N_b^2$, respectively). This suggests that we should consider the folding in of a *single* arm, as proposed by de Gennes (Figure 1), as a dynamic process, obeying a diffusion equation similar to eq III.7. The origin of the force opposing the folding back of a chain onto itself without enclosing any obstacles (Figure 1b) is similar to that opposing the motion of the center monomer C up a tube (Figure 5b). The gain in free energy $\delta U = T\Delta S$ when the end of an arm advances one step back onto itself, so that the total length of the arm in the non-obstacle-enclosing fold (Figure 1b) goes from $q_1 \rightarrow q_1 + 1$ primitive steps, is given by

$$U = T[S(P_1(q_1)) - S(P_1(q_1-1))] = kT[\ln(P_1(q_1)) - \ln(P_1(q_1-1))] \simeq \alpha kT \quad \text{(III.12)}$$

where we have again used for simplicity the approximate (purely exponential) form of $P_1 = P_1'$ (eq I.2). This results in a potential field opposing the folding back of an arm of the form

$$U(q_1) = \alpha|q_1|kT \quad \text{(III.13a)}$$

The *length* of tube occupied by a fold of $q_1$ steps is $x_1 = (q_1/2)\xi$, so that we may write the potential field

$$U(x_1) = 2\alpha|x_1|kT \quad \text{(III.13b)}$$

The diffusion equation for the folding up of a *single* arm then has exactly the same form as (III.7) but with different conditions. The solution for the expectation time (or first passage time) for $q_1 \rightarrow N_b$, or $x_1 \rightarrow N_b\xi/2$, is $\langle\tau\rangle \equiv \tau_{s1}$, and the corresponding diffusion coefficient $D_{s1} \simeq \xi^2/\tau_{s1}$ is similar to that for $\tau_{s2}$ and $D_{s2}$. We find (Appendix I)

$$\tau_{s1} = (\tau_{rep}(n_b)/8\alpha^2N_b^2)e^{\alpha N_b} \qquad f = 3 \quad \text{(III.14)}$$

$$D_{s1} = 8\alpha^2N_bD_{rep}(n_b)\exp(-\alpha N_b) \qquad f = 3 \quad \text{(III.15)}$$

For the case of $f > 3$, the center monomer can take a stochastic step only when $(f-2)$ arms together retract as shown in Figure 1. The main effect of this is to increase the exponent in eq III.14 and III.15 by a factor $(f-2)$; there is also an effect on the preexponential factor (through a weak $f$ dependence). The main difference between the expectation times for a topological step associated with the single-arm retraction and a fixed center, (Figure 1 and eq III.14) and that associated with a moving center and no arm retraction (Figure 5, eq III.10) is the higher exponent in the latter case, implying a much slower relaxation at large arm length $N_b$.

More generally, one might expect the basic diffusion step (in a fixed topology of obstacles) to take place by a *combination* of the configurations shown in Figures 1 and 5, as indicated in Figure 6 ($f = 3$ for clarity): the center

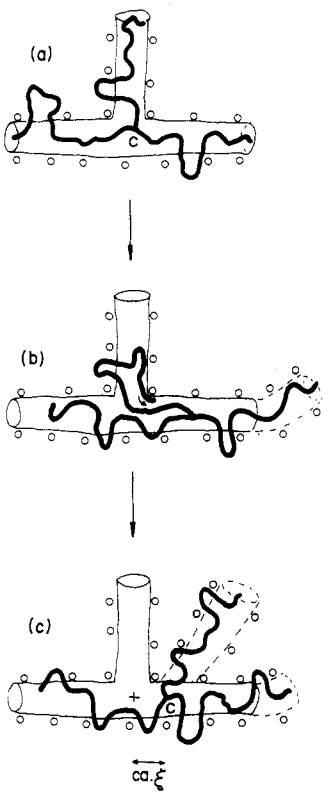


**Figure 6.** A diffusion step taking place by a combination of the processes illustrated in Figures 1 and 5: the center monomer C moves partly down an arm ($q_2$ steps) and the remaining ($N_b - q_2$) steps of ($f - 2$) = 1 (in this case where $f$ = 3) of the other arms now retract (b) to allow C to make a step of size $\xi$ (c).

monomer moves $q_2$ steps down one of the arm tubes, dragging the other ($f - 1$) arms with it, and ($f - 2$) of the remaining arms then "retract" ($N_b - q_2$) steps each, as in Figure 6b. The motion of the end of an arm is then described by a *coupled* diffusion equation

$$\left[\frac{\partial}{\partial t} - D_1\frac{\partial}{\partial x_1}\left(\frac{\partial}{\partial x_1} + \frac{1}{kT}\frac{\partial U(x_1,x_2)}{\partial x_1}\right) - D_2\frac{\partial}{\partial x_2}\left(\frac{\partial}{\partial x_2} + \frac{1}{kT}\frac{\partial U(x_1,x_2)}{\partial x_2}\right)\right]P(x_1,x_2,t) = 0 \quad \text{(III.16)}$$

where $x_1$ and $x_2$ are the fold length (of a retracted arm) and the distance moved by the center monomer up a tube, respectively (Figure 6), $D_1$ and $D_2$ are the respective diffusion coefficients (equal to $kT$/friction coefficient) associated with such motion, and $P(x_1,x_2,t)\ dx_1\ dx_2$ is the probability of a configuration $(x_1,x_1+dx_1)$, $(x_2,x_2+dx_2)$. A topological step may be taken whenever $q_1$ (the number of primitive steps in a fold) and $q_2$ (the number of steps moved up a tube) obey

$$q_1 + q_2 = N_b \quad \text{(III.17)}$$

The expectation time for this to happen is evaluated (using an adiabatic procedure) in Appendix II and is given by

$$\tau_s = (\tau_{rep}(n_b)/12\alpha^2N_b^2)\exp(\alpha N_b) \qquad f = 3 \quad \text{(III.18)}$$

with a corresponding diffusion coefficient $D_s \simeq \xi^2/\tau_s$

$$D_s = 12\alpha^2N_bD_{rep}(n_b)\exp(-\alpha N_b) \qquad f = 3 \quad \text{(III.19)}$$

Comparison of the expectation times $\tau_{s1}$ (eq III.14) and $\tau_s$ (eq III.18) shows that allowing the center monomer to move as in Figure 6 makes little difference in the expectation time for a topological step relative to that for arm retraction with a fixed center (Figure 1): the latter process

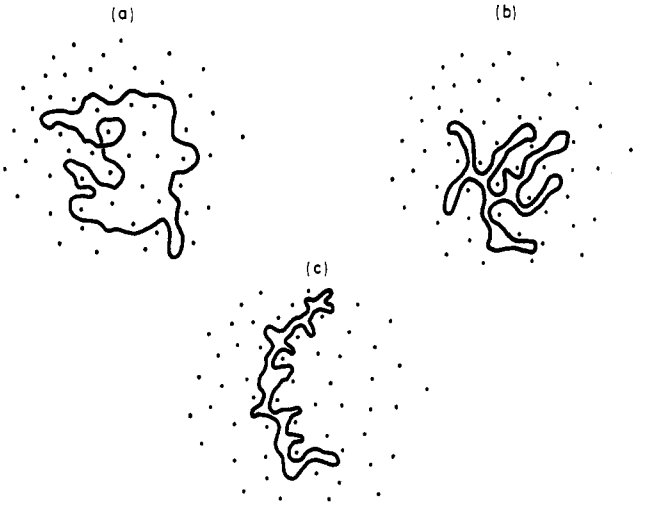


**Figure 7.** Possible configurations for a ring polymer in a matrix of noncrossable obstacles (sections through which are represented by black points): (a) general, obstacle-enclosing; (b) non-obstacle-enclosing, but ramified, i.e., large loops; (c) non-obstacle-enclosing, nonramified (small loops only).

(for a three-arm star in the limit of long arms in our model) takes 50% longer.

An interesting feature emerges when we consider the relevant longest relaxation times $\tau$ for *stress relaxation* (related to steady-flow viscosity as $\eta_0 \propto \tau/n_b$) for a single star molecule in essentially fixed surroundings. For a *fixed* center monomer, $\tau$ is simply given by $\tau_{s1}$ as in eq III.14; for a more general mode of motion, for a *three-armed star* ($f$ = 3), the relaxation time is shortened, by the availability of additional relaxation modes (Figure 6), to the value $\tau_s$ given in (III.18). However, *for $f > 3$*, the probability of a center monomer dragging ($f - 1$) arms up a tube (Figure 5c) decreases rapidly, (e.g., eq III.2, III.10, and III.11), and, especially for long arms, the contribution of processes as shown in Figures 5 and 6 (for $f > 3$) becomes negligible. Nevertheless, even for $f > 3$ a star may still undergo stress relaxation by single-arm processes, shown in Figure 1, with a relaxation time $\tau_{s1}$ (eq III.14) as the $f$ arms relax independently and without need for cooperativity. The conclusion is that the relaxation time of *three-arm* stars in a fixed environment (e.g., a star melt—see later) is shorter—for a given arm length—by about $^1/_3$ than the corresponding time for $f$-armed stars with $f > 4$. Steady-flow viscosities for three-arm stars should be correspondingly lower than for $f \geq 4$ for a given arm length. This is a small but systematic effect, though we are not aware whether experimental evidence in star melts supports this prediction.[43]

We should note that for center of mass *translational diffusion*, cooperativity of arms *is* required, and $D_s$ falls rapidly with $f$

$$D_s \simeq \alpha^2N_bD_{rep}(n_b)\exp[-\alpha(f-2)N_b] \qquad f \geq 3 \quad \text{(III.19')}$$

omitting a weak preexponential $f$ dependence.

**Closed Cyclic Polymers.** Closed *cyclic* polymers in a fixed obstacle lattice may either be pinned by obstacles, as in Figure 7a, or be "unpinned" in the sense indicated in Figure 7b, where the closed cyclic or ring polymer does not enclose any obstacles (this possibility was ignored in an earlier treatment[26]). Clearly if pinned, as in Figure 7a, the ring molecules may not undergo translational diffusion in the usual sense (reptative motion will not "untrap" the ring but merely rotate it about its mean position). The probability of unpinned configurations as in Figure 7b is low and may be estimated as follows. The probability that

an $N_R$-step, *linear* random walk has an end-to-end distance $r$ is given by the usual Gaussian expression

$$P(r) = (\text{const}/N_R^{3/2}) \exp[3r^2/2N_R\xi^2] \quad \text{(III.20)}$$

(where $\xi$ is the step size) so that the probability that the ends of the walk meet, $r = 0$, is simply

$$P(0) = \text{const}/N_R^{3/2} \quad \text{(III.21)}$$

The probability that the ends meet and the linear $N_R$-step walk in addition goes back to the start without enclosing any obstacles is given by eq III.3[22,24]

$$P_1(N_R) = (\text{const}/N_R^{3/2})e^{-\gamma N_R} \quad \text{(III.22)}$$

For a ring molecule, however, which may be considered as a closed linear random walk, the probability that its "ends" meet is clearly unity. By comparison of (III.21) and (III.22), therefore, we deduce the form of the probability that a closed cyclic $N_R$-step walk does not enclose any obstacles as simply

$$P_R(N_R) = (\text{const})e^{-\gamma N_R} \quad \text{(III.23)}$$

The translational diffusion coefficient of that part of the ring population that is unpinned (Figure 7b) depends on whether the doubled-up configuration is ramified, Figure 7b, or essentially *linear*, Figure 7c. The probability $P_R^L(N)$ of the latter case is lower than $P_R(N_R)$ (eq III.23), which includes all possible ramifications as in Figure 7b. We may roughly estimate it (Appendix III) as

$$P_R^L(N_R) \simeq (\text{const})e^{-\beta N_R} \quad \text{(III.24)}$$

where $\alpha \lesssim \beta \lesssim 2\alpha$ (Appendix III). When it is effectively linear, the ring polymer will be able to diffuse by *reptation*, with a diffusion coefficient $D_R^L$ given by

$$D_R^L(N_R) \simeq D_{rep}(N_R/2) \quad \text{(III.25)}$$

the diffusion coefficient of a reptating linear $(N_R/2)$-step polymer (within a factor of order 2). The ring polymers with ramified structures (as in Figure 7b) will in general have lower diffusion coefficients (in analogy with star-branched molecules, for example); it may be shown that their overall contribution to the diffusion of the ring polymer population will be comparable with $D_R^L$, but at this level of sophistication we retain only the latter (III.25).

We may define a relaxation time for a ring in a fixed obstacle environment by considering *only non-obstacle-enclosing rings* as in Figure 7c. A characteristic time is then given by

$$\tau_R(N_R) \simeq R^2(N_R)/D_R^L(N_R) \quad \text{(III.26)}$$

where $R(N_R)$ is the size (tip-to-tip) of an $N_R$-step ring; we stress that this time is characteristic only of that small part of the overall polymer population having zero topology (nonramified, as Figure 7c).

It is important to bear in mind that the expressions used for the various probabilities only apply in the limit of large $N_R$. At low $N_R$ values the probability of ring configurations that are *non-obstacle enclosing* is much higher than $P_R(N_R)$ (eq III.23) and may even account for the majority of all possible configurations. To get an estimate of how long an entangled ring needs to be in order for the probability limit $P_R(N_R)$ to be approached, we proceed as follows: the total number of configurations of an $N_R$-step ring on a $z$-coordination lattice is just

$$Q(N_R) = P(0)z^{N_R} \quad \text{(III.27)}$$

with $P(0)$ given by (III.21) ($N$ large). The number of configurations not enclosing any obstacles is

$$Q_R(N_R) = P_R(N_R)z^{N_R} \quad \text{(III.28)}$$

with $P_R(N_R)$ as in (III.23) ($N_R$ large). At $Q(N_R^+) \simeq 2Q_R(N_R^+)$, the number of obstacle-enclosing and non-obstacle-enclosing ring configurations are comparable. Using the large $N_R$ limits for both $P(0)$ and $P_R(N_R)$ to get a first estimate of $N_R^+$, we have (on substituting for the two probabilities)

$$2e^{-\gamma N_R^+} \simeq (N_R^+)^{-3/2} \quad \text{(III.29)}$$

which gives (with the more detailed normalization constants[22,24] in $P(0)$ and $P_R(N_R)$ and on putting $\gamma = \alpha \simeq 0.6$–$0.7$, Appendix III)

$$N_R^+ \simeq 8\text{–}10 \quad \text{(III.30)}$$

Thus for ring lengths of up to about $N^+ = 10$ entanglement lengths a considerable proportion (of order 50% or more) of the ring population in an entangled melt may be non-obstacle-enclosing. For $N_R \gg N_R^+$ this proportion rapidly approaches the limit $P_R(N_R)$.

## IV. Star and Ring Polymers in a Linear $p$-mer Melt

A central assumption in considering the behavior of entangled star and ring polymers in a linear polymer melt is that their motion will be a combination of the two (independent) extremes treated in the previous sections, that is, curvilinear motion in fixed "tubes" and a general (Rouse–Zimm type) motion controlled by the relaxation of the "tubes" themselves. The transition between the two types of behavior will be characterized by certain *crossover dimensions* of the nonlinear molecules.

We shall make use of the fact that the diffusion coefficient and longest relaxation time for an ideal $f$-arm, $n_b$-mer/arm star are essentially identical with those of a $2n_b$-mer linear molecule in both the screened (Rouse) and unscreened (Zimm) limits,[34] while for an ideal $n_R$-mer ring molecule the dilute solution diffusion coefficient and longest relaxation times are closely similar (within a factor of 3) to those of a linear $n_R$-mer in both limits.[35]

**Stars.** For a symmetric $fn_b$-mer star in a linear $p$-mer melt we shall have an overall diffusion coefficient given by the sum for the two processes

$$D_s(f,n_b,p) = D_s(f,N_b) + D_{tube}(2N_b) \quad \text{(IV.1)}$$

with $D_s(f,N_b)$ given by (III.19′); $D_{tube}(2N_b)$ is given either by (II.13) for Rouse-like behavior ($n_b \lesssim n^{**}$) or by (II.22) for $n_b \gg n^{**}$ (Zimm-like tube renewal). At low $n_b$ values the exponentially suppressed reptation coefficient $D_s$ applies, while for larger arm lengths tube renewal is the dominant mode. The crossover will occur at $n_b^*$, where

$$D_s(f,N_b^*) = D_{tube}(2N_b^*) \quad \text{(IV.2)}$$

where $N_b^* = (n_b^*/n_c)$. Assuming Rouse-like tube renewal and substituting from (III.19) and (II.13), we have

$$\alpha^2 N_b^* D_{rep}(n_b^*) \exp[-\alpha N_b^*(f-2)] = N_b^* p_c^{1/2} P^{-5/2} D_{rep}(n_b^*) \quad \text{(IV.3)}$$

dropping small numerical prefactors as usual. Taking $p_c$ to be 100 monomers, a typical value for synthetic linear polymers, and $\alpha$ as 0.6–0.7 (a value suggested both by lattice calculations and by fitting to viscoelastic date),[22,25] we find

$$N_b^* \simeq \frac{2\text{–}16}{(f-2)} \quad \text{(IV.4)}$$

for $p$ in the usual range 3–200 entanglement lengths. Because of the exponent in (IV.3), the crossover value $N_b^*$

is not very sensitive to the numerical prefactors (which were dropped from (IV.3)).

We note that, at the crossover, (i) $n_b^* \ll n^{**}$ (eq II.19), implying that Rouse tube renewal self-consistently applies, and (ii) there is considerable interdependence of $p$ neighbors about the $n_b^*$-arm; i.e., even at the largest $p$ values, $p^{1/2} \ll n_b^*$, so that the enhanced relaxation rate $1/\tau_c$ (eq II.9) should apply.

The longest relaxation rate for the star, $1/\tau_s(f,n_b,p)$, is likewise a sum of the rates for "fixed-tubes" and tube-renewal mechanisms

$$[\tau_s(f,n_b,p)]^{-1} = \tau_s^{-1} + [\tau_{tube}(2N_b)_R]^{-1} \quad \text{(IV.5)}$$

with the two terms on the right-hand side given by (III.18) and (II.12), respectively. We recall that $\tau_s$ (for $f > 3$) is essentially the relaxation time of a single arm (there is no need for cooperativity between arms, as is the case for diffusion), so that $\tau_s(f,n_b,p)$ is independent of $f$ for a given arm length. The crossover from suppressed reptation ($\tau_s$) to tube renewal occurs for $n_b$ greater than some value defined by the equality of the two right-hand side terms of (IV.5). Substituting from (III.18) and (II.12), we find this value to equal $n_b^*$ (eq IV.4) at $f = 3$.

**Rings.** A population of ring $n_R$-mers in equilibrium with a linear $p$-mer melt will have a fraction $P_R^L(N_R)$ (eq III.24) of its members in an essentially linear configuration (Figure 7c) at any one time ($N_R$ large); if only these molecules are able to participate in translational diffusion processes (e.g., when $p$ is large so that the entangling environment is to all intents and purposes fixed), then we expect the effective diffusion coefficient for the sample to be approximately

$$D_R(n_R) \simeq P_R^L(N_R) D_R^L(N_R) \simeq D_{rep}(n_R) e^{-\beta N_R} \quad \text{(IV.6)}$$

(since each molecule spends a fraction $P_R^L(N_R)$ of its time in a "reptating configuration"), where $D_{rep}(n_R)$ is the reptation diffusion coefficient of the corresponding linear $n_R$-mer. Then the overall diffusion coefficient for the ring, taking tube renewal into account, is

$$D(n_R,p) \simeq D_R(n_R) + D_{tube}(N_R)_R \quad \text{(IV.7)}$$

with a crossover from essentially curvilinear diffusion to tube-renewal dynamics at $N_R^*$, given at the equality of the two right-hand-side terms in (IV.7). Substituting from (IV.7) and (II.13), we find (taking $\beta = 1$, Appendix III)

$$N_R^{*\prime} \simeq 2\text{–}10 \quad \text{(IV.8)}$$

for the range of linear polymer sizes $p = 5$–$200$ entanglement lengths. Since these crossover values are smaller than or comparable with $N_R^+$ (eq III.29), it is incorrect to use the large-$N_R$ limit expression for $D_R(n_R)$. At $N_R < N_R^+$ a substantial proportion of the ring population is non-obstacle-enclosing and may undergo pure reptative motion—in this case the effect of tube renewal is weak, as discussed in section II. However, the implication of the low values of $N_R^*$ is that tube renewal will be dominant (for a ring in a linear melt) already at $N_R \gtrsim N_R^+$ and that exponentially suppressed reptation will thus be observed only over a rather limited $N_R$ range. Rather, the diffusion will proceed by normal reptation

$$D(n_R,p) \simeq D_{rep}(n_R), \qquad N_R \lesssim N_R^+ \quad \text{(IV.9)}$$

or by tube renewal

$$D(n_R,p) \simeq D_{tube}(N_R)_R, \qquad N_R > N_R^+ \quad \text{(IV.10)}$$

Similar considerations apply to the largest relaxation time $\tau_R(n_R,p)$ of the ring $n_R$-mer in a linear $p$-mer melt, which is given by

$$\tau_R^{-1}(n_R,p) \simeq \tau_R^{-1}(n_R) + \tau_{tube}^{-1}(N_R)_R \quad \text{(IV.11)}$$

where

$$\tau_R(n_R) \simeq R^2(n_R)/D_R(n_R) \quad \text{(IV.12)}$$

The crossover value at which the two right-hand side terms of (IV.11) are equal is the same as $N_R^{*\prime}$ (IV.8) and is lower than or comparable to $N_R^+$; this implies, as for diffusion, that at $N_R \lesssim N_R^+$ one expects relaxation by essentially reptative processes, with times

$$\tau_R(n_R,p) \simeq \tau_{rep}(n_R), \qquad N_R \lesssim N_R^+ \quad \text{(IV.13)}$$

and tube-renewal dominance for longer rings

$$\tau_R(n_R,p) \simeq \tau_{tube}(N_R)_R, \qquad N_R \gg N_R^+ \quad \text{(IV.14)}$$

Exponentially suppressed reptative relaxation, $\tau_R(n_R)$ (eq IV.12), will therefore be effectively be bypassed (or may dominate over a narrow range $N_R \gtrsim N_R^+$) in the mixed ring/linear system. In a melt of rings, however, where tube renewal may be a negligible process, both $D_R(n_R)$ and $\tau_R(n_R)$ may be the relevant processes for large $N_R$ ($\gg N_R^+$).

To summarize: $n_R$-mer rings in a $p$-mer linear melt will diffuse and relax by approximately normal reptative motion for $n_R \lesssim n_R^+$ ($=N_R^+ n_c$) and then by exponentially suppressed reptation over a narrow range $N_R^+ \lesssim N_R \lesssim N_R^*$ (where $N_R^*$ is somewhat greater than $N_R^+$); at $N_R \gg N_R^+$ the ring motion will be dominated by Rouse-like tube-renewal processes.

## V. Discussion and Conclusions

We have treated the dynamics of entangled linear and nonlinear $n$-molecules in entangled linear $p$-melts as a combination of two independent modes: reptation within a fixed topological environment (fixed "tubes") and a general nonreptative motion due to the relaxation of topological constaints (tube renewal); transitions between the regimes are characterized by certain crossover dimensions of the $n$-mers.

An important modification to earlier models of tube renewal is our conjecture that the release rate of the effective constraints defining a tube is considerably enhanced (by $\sim p^{1/2}$) as a result of the nonindependence of the $p$-mer segments adjacent to an entangled $n$-mer, as discussed in section III. This is a strong assumption; it would not apply, for example, if such effective tube constraints consisted of individual uniquely entangling molecules $p_c$-mers apart: in this case the enhancement would be of the order $(p^{1/2}/p_c) \lesssim 1$, unimportant for the normal range of polymer sizes. The main implications of the more rapid constraint release are (i) that the tube-renewal contribution to the relaxation and diffusion process (for an $n$-mer in a $p$-mer matrix) varies as

$$\tau_{tube} \sim n^2 p^{5/2} \quad \text{(V.1)}$$

$$D_{tube} \sim n^{-1} p^{-5/2} \quad \text{(V.2)}$$

and (ii) tube-renewal processes are hydrodynamically screened (Rouse-like) up to high $(n/p)$ values, beyond which hydrodynamic interactions become important (Zimm-like). The latter regime is explicitly identified with the Stokes–Einstein hydrodynamic sphere limit noted by Daoud and de Gennes, but the $n^{**}$ values at which it is attained may be too high to be observed for the usual range of polymers available. Equations V.1 and V.2 are the "free-draining" (Rouse-like) tube-renewal values.

Two very recent studies have probed tube-renewal processes in linear melts. Measurements by the Pau group[36] of the viscosity of binodal ($n$-mer in $p$-mer) polystyrene blends suggest a tube-renewal contribution to the $n$-mer relaxation that is not too far from (V.1). On the other hand, experiments by the Cornell group[14] using

nuclear scattering techniques to measure the diffusion of deuterated polystyrene $n$-mers in a protonated $p$-mer polystyrene matrix indicate

$$D \propto n^{-1}p^{-3} \tag{V.3}$$

in a regime where tube renewal dominates. The range of $p$ within this regime is relatively narrow, however, and the results may also be consistent (within the scatter) with the prediction (V.1). The matrix size $p^*$ below which—for a given $n$—tube renewal is observed in these diffusion experiments is comparable with the values estimated in section II (i.e., $p^* \simeq (np_c^2)^{2/5}$, from eq II.14).

**Stars.** Treating the entangled star ($f$-arms, $n_b$/arm) motion in terms of a generalized diffusion process (coupled arm retraction and center motion) in an entropic potential field does not change the essential exponentially suppressed relaxation and diffusion rates proposed in earlier treatments.[5,20-23] The preexponential arm-length ($n_b$) dependence of both $D_s$ and $\tau_s$ does change, but at high $n_b$ values the behavior is dominated by the exponential. Recent diffusion studies[27] of three-arm deuterated polybutadiene stars in a fixed, high-molecular-weight, chemically identical linear melt do seem to show a power-exponential behavior that is a rather good fit to the form

$$D_s \propto (1/n_b)e^{-\alpha N_b} \tag{V.4}$$

calculated in section III. At the highest $n_b$ values in this study the dependence of $D_s$ on $n_b$ becomes much weaker, strongly suggesting tube-renewal dominance, though the data does not extend far enough in $n_b$ to discriminate between an $n_b^{-1/2}$ (Zimm-like) or an $n_b^{-1}$ (Rouse-like) dependence in the tube-renewal regime. The crossover values $n_b^*$ for diffusion by tube renewal of $n$-mers in linear $p$-mer melts are much lower than for linear molecules, and such studies should provide more readily experimentally feasible checks of tube-renewal mechanisms. The actual value of $n_b^*$ in the star diffusion studies[27] appears lower (by a factor of 2 or so) than the estimates of section IV for such a system, though we note that the polydisperse nature of the linear-melt matrix used makes difficult any assignment of a value for $p$.

In the computer simulation study by Needs and Edwards[24] of entangled three-arm stars diffusing in a fixed obstacle matrix, power–exponential relations were indicated for both the center of mass diffusion ($D_s$) and the relaxation time ($\tau_s$), with best fits

$$D_s \propto N_b^{-0.6} \exp(-B_1N_b) \tag{V.5}$$

and

$$\tau_s \propto N_b^{1.9} \exp(B_2N_b) \tag{V.6}$$

The $N_b$ exponents in the preexponential factors indicated for both $D_s$ and $\tau_s$ are slightly different from those calculated (for the high $N_b$ limit) in section III, (−0.6 vs. −1 for $D_s$ and 1.9 vs. 1 for $\tau_s$); it is not clear whether this is due to a deficiency in the model or to a nonattainment of a sufficiently large $N_b$ range or extent of center-of-mass motion in the simulation experiment. It is of some interest in the context of the computer simulation, where the center monomer of the star is allowed to move, that on *fixing* the center monomer the star relaxation time increased by between 20% and 80% relative to an unfixed center, and this increase in $\tau_s$ was independent of $N_b$.[24] This compares with our calculated increase in $\tau_s$ by 50% (also independent of $N_b$), when the center monomer is fixed (eq III.14) relative to a free center monomer (eq III.18).

The relaxation process in *melts* of stars may also be treated in terms of two independent contributions. However, the tube-renewal component in a star melt is clearly much slower than for a star in a linear melt—one expects the effective constraint relaxation rate to be (self-consistently) exponentially suppressed at high $N_b$. The resulting relaxation times and diffusion coefficient for sufficiently large $N_b$ are given by the corresponding "fixed-tube" values, and one expects the zero shear rate viscosity $\eta_{os}(f,N_b)$ of such a melt to scale as the single-arm relaxation time $\tau_{s1}(N_b)/n_b$. Similar conclusions (with different power dependences on the arm length but always with the dominant exponential term) have been reached earlier; we recall however our conjecture (section III) that $\eta_{os}(3,N_b) \simeq {}^2/_3\eta_{os}(f,N_b)$ for $f > 3$.[43]

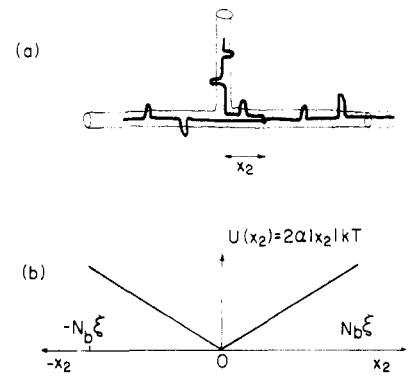


**Figure 8.** (a) Schematic representation of motion of center monomer a distance $x_2$ up an arm tube with (b) the corresponding potential $U(x_2)$. The motion of the star center is governed by a diffusion equation of a particle under Brownian motion in the potential $U(x_2)$.

One final comment is in order; the activation energy $Q_{VS}$ for the viscosity of entangled star melts is found to be higher for some polymers (e.g., hydrogenated PBD) than $Q_{VL}$ for the corresponding linear melts,[37] and in addition the difference varies with the arm length $N_b$. Furthermore, in a very recent study, the activation energy $Q_{DS}$ for the *translational diffusion* of three-arm polyethylene-like stars (in a highly entangled linear-melt matrix) was measured[27] and found to be higher than both $Q_{DL}$ (for diffusion of the corresponding linear polymer) and $Q_{VS}$ (for the same number of arms and $N_b$). Whatever the molecular origin of these differences,[37] it is important to take them into account in comparison of viscosity and diffusion data between star and linear polymers, as well as in the intepretation of the variation of these dynamic quantities with $N_b$ for melts of homologous stars.

**Rings.** Preliminary experimental data on diffusion and viscosity in entangled ring melts (and rings in linear melts) have only very recently been reported,[38,39] though they should become more available in coming years.[44] Our discussion of diffusion and relaxation of entangled ring $n_R$-mers has been less detailed than for stars; at sufficiently high $n_R$ one expects exponentially suppressed reptation and relaxation for "fixed" tubes (or ring melts, for example)

$$D_R \sim e^{-\beta N_R} \tag{V.7}$$

$$\tau_R \sim e^{\beta N_R} \tag{V.8}$$

omitting power-dependent prefactors (where the constant $\beta$ is comparable with the corresponding exponential factor for stars). For rings in linear melts, tube renewal soon takes over.

It is important to note that the limiting forms (V.7) and (V.8) strictly apply only at $N_R$ ($=n_R/n_e$) $\gg N_R^+$, where $N_R^+$ is of order 10 (entanglement lengths): for ring sizes lower than or comparable with $N_R^+$, there is an appreciable probability of rings not enclosing any entanglements (for

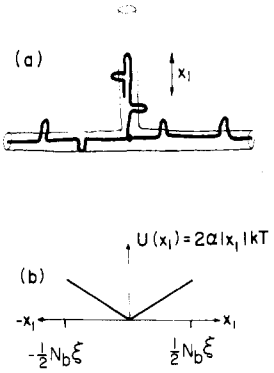


**Figure 9.** (a) Representation of arm retraction, with a fold length $x_1$ along the tube, and (b) the corresponding potential $U(x_1)$. The motion of the arm tip is governed by the diffusion equation of a particle in the potential $U(x_1)$.

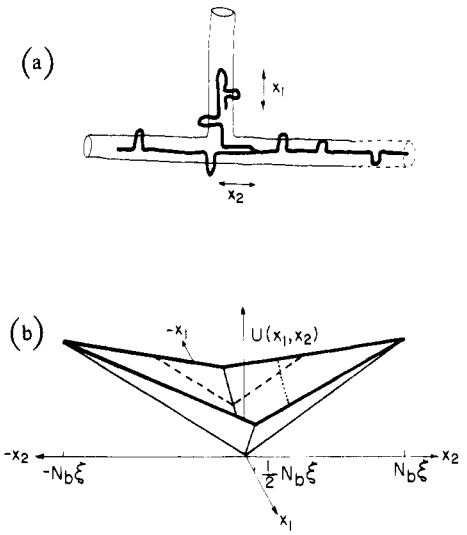


**Figure 10.** (a) Combination of the motions in Figures 8 and 9. The resultant motion may be represented as diffusion of a particle on the inside walls of an upturned pyramid as shown in (b), subject to a potential $U(x_1,x_2)$ that is the height of the pyramid walls at $(x_1,x_2)$ above the $x_1$–$x_2$ plane (eq AII.1).

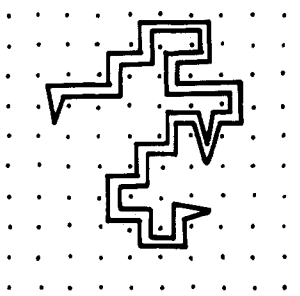

**Figure 11.** An $N_R$-step random walk on an obstacle lattice, taking $N_R/2$ steps at random and retracing them exactly with the remaining $N_R/2$ steps, approximates a nonramified, non-obstacle-enclosing ring as in Figure 7c.

the reasons discussed in section III); their behavior is then expected to be qualitatively similar to that of entangled *linear* molecules. The overall diffusion and relaxation of rings of intermediate lengths (straddling the value $N^+$) will then be a combination of pure reptative motion, exponentially suppressed reptation, and tube-renewal effects. This implies that interpretations of experimental data in terms of molecular relaxation mechanisms are probably best carried out for the range $N_R \gtrsim 2N_R^+$, where the limiting relations (V.7) and (V.8) (or the appropriate tube-renewal expressions in the case of a linear $p$ matrix) should apply.

**Acknowledgment.** This paper was written in part while I was working at the Cavendish Laboratory, and I would like to thank S. F. Edwards and R. Ball for useful discussions and particularly for their help in solving the diffusion equation (Appendix I). I have also greatly benefited from discussions, release of data prior to publication, and correspondence on related topics with Z. Alexandrowicz, J. Deutsch, M. Doi, J. D. Ferry, L. J. Fetters, P.-G. de Gennes, W. W. Graessley, E. Helfand, A. Kovacs, E. J. Kramer, D. S. Pearson, J. Roovers, and A. Silberberg. Several fruitful ideas emerged in discussions during a visit to Pau, and I am grateful to Ph. Monge, J.-P. Montfort and G. Marin for discussions (especially concerning tube-constraint interdependence) and for their kind hospitality on that occasion.

## Appendix I

The form of the potential $U(x_2)$ is illustrated in Figure 8. The motion of the center monomer C in this potential is given by eq III.7, which may be rewritten as

$$\partial P(x_2,t)/\partial t = \mathcal{L}(x_2)P(x_2,t) \qquad \text{(AI.1)}$$

where the operator

$$\mathcal{L}(x_2) \equiv D_2\frac{\partial}{\partial x_2}\left(\frac{\partial}{\partial x_2} + \frac{1}{kT}\frac{\partial U}{\partial x_2}\right)$$

Define

$$\tau(x_2) = \int_{t=0}^{\infty} P(x_2,t)\,dt \qquad \text{(AI.2)}$$

so that the first passage time (i.e., the expectation time for C to "escape" at $x_2 = \pm N_b\xi$) is

$$\langle\tau\rangle = \int_{x_2=-N_b\xi}^{+N_b\xi} \tau(x_2)\,dx_2 \qquad \text{(AI.3)}$$

Now operate $\int_0^\infty dt$ on both sides of (AI.1)

$$\int_0^\infty \frac{\partial P}{\partial t}\,dt = \mathcal{L}(x_2)\int_0^\infty P(x_2,t)\,dt \qquad (2)$$

giving

$$P(x_2,\infty) - P(x_2,0) = \mathcal{L}(x_2)\tau(x_2)$$

Since $P(x_2,\infty) = 0$, this gives (on operating $\mathcal{L}$)

$$D_2\frac{\partial}{\partial x_2}\left(\tau' + \frac{\tau}{kT}U'\right) + P(x,0) = 0 \qquad \text{(AI.4)}$$

where primes are derivatives with respect to $x_2$. $P(x,0)$ is the equilibrium probability of finding the center monomer C a distance $(x_2,x_2+dx_2)$ up one of the arm tubes, which is given by a Boltzmann distribution

$$P(x_2,0) = Ae^{-U(x_2)/kT}$$

where the normalizing constant $A$ is

$$A = \int_{-N_b\xi}^{N_b\xi} \exp[-U(x)/kT]^{-1}\,dx \simeq \frac{\alpha}{\xi} \qquad \text{for } N_b \gg 1$$

The boundary conditions on eq AI.4 are $\tau(-N_b\xi) = \tau(N_b\xi) = 0$. The solution to eq AI.4 for $\tau$ is straightforward (though care must be taken because of the cusp at the origin), giving

$$\tau(x_2) = \frac{A\xi^2}{4\alpha^2D_2}(e^{2\alpha(N_b\xi-x_2)/\xi} - 1) - \frac{A\xi}{2\alpha D_2}e^{2\alpha x_2/\xi}(N_b\xi - x_2) \qquad \text{(AI.5)}$$

for $x_2 \geq 0$, with a similar form (but letting all $x_2 \geq -x_2$) for $x_2 \leq 0$.

Then the first passage time is

$$\langle\tau\rangle = \int_{-N_b\xi}^{N_b\xi} \tau(x_2)\, dx_2$$

and has a dominant term, for $N_b \gg 1$

$$\langle\tau\rangle \simeq \left(\frac{\xi}{\alpha}\right)^2 \frac{1}{4D_2} e^{2\alpha N_b} \qquad \text{(AI.6)}$$

on substituting for $A$.

As the motion is within tubes and involves $f$ arms of the molecule (where $f = 3$ has been assumed in the calculation (i.e., $U = (2\alpha/\xi)(f-2)|x|kT \equiv (2\alpha/\xi)|x|kT$ for $f = 3$) we expect $D_2$ to equal the curvilinear diffusion coefficient of an $fn_b$-mer linear molecule

$$D_2 = D_c(fn_b) = \frac{n_b{}^2 l^2}{2fn_c\tau_{rep}(n_b)} \qquad \text{(AI.7)}$$

from eq II.3–II.5. On substituting in (AI.6), we have

$$\langle\tau\rangle = \frac{f}{2\alpha^2 N_b{}^2}\tau_{rep}(n_b)e^{2\alpha(f-2)N_b} \qquad \text{(AI.8)}$$

where $2\alpha \to 2\alpha(f-2)$ in the exponent for a general $f \geq 3$. This is the value of $\tau_{s2}$ given in eq III.10 in the text.

For the *single*-arm retraction, with a fixed center, the diffusion equation (in this case for motion of the *tip* of an arm, in the potential field $U(x_1) = (2\alpha/\xi)|x_1|kT$) is very similar to eq III.7 and has the form

$$\left(\frac{\partial}{\partial t} - D_1\frac{\partial}{\partial x_1}\left(\frac{\partial}{\partial x_1} + \frac{\partial U(x_1)/\partial x_1}{kT}\right)\right)P(x_1,t) = 0 \qquad \text{(AI.9)}$$

where $U(x_1)$ has the form shown in Figure 9 and $D_1$ is the diffusion coefficient associated with the curvilinear motion for folding the *single arm*. The other difference from the equation for $P(x_2,t)$, eq III.7 or AI.1, is that the boundary conditions are now $P(x_1,t) = 0$ at $x_1 = \pm N_b\xi/2$, since a topological step may be taken when the length $x_1$ of the folded configuration is *half* of an arm length $N_b\xi$ (Figure 9).

The procedure for solving (AI.9) is identical with that for solving (AI.1) and gives an expectation time whose dominant term (for $N_b \gg 1$) is

$$\langle\tau\rangle = \left(\frac{\xi^2}{8\alpha^2}\right)\frac{1}{D_1}e^{\alpha N_b} \qquad \text{(AI.10)}$$

Putting

$$D_1 = D_c(n_b/2) \qquad \text{(AI.11)}$$

and substituting from eq II.3–II.5, we find

$$\langle\tau\rangle_1 = \frac{\tau_{rep}(n_b)}{8\alpha^2 N_b{}^2}e^{\alpha N_b}$$

which is the expression for $\tau_{s1}$, eq III.14.

## Appendix II

The general mode for the basic diffusion step shown in Figure 6 is reproduced schematically in Figure 10 and obeys the coupled diffusion eq III.16

$$\left[\frac{\partial}{\partial t} - D_1\frac{\partial}{\partial x_1}\left(\frac{\partial}{\partial x_1} + \frac{1}{kT}\frac{\partial U}{\partial x_1}\right) - D_2\frac{\partial}{\partial x_2}\left(\frac{\partial}{\partial x_2} + \frac{1}{kT}\frac{\partial U}{\partial x_2}\right)\right]P(x_1,x_2,t) = 0 \qquad \text{(AII.1)}$$

It is instructive to draw the form of the potential $U(x_1,x_2)$ associated with the configuration $(x_1,x_2)$: this can be represented as an upturned four-sided pyramid with edges parallel to orthogonal $x_1$, $x_2$ axes (Figure 10) and its vertex at the origin (0,0). The motion represented by eq III.16 is that of a point moving by Brownian motion on the inside walls of the pyramid subject to the potential

$$U(x_1,x_2) = U(x_1) + U(x_2) = (2\alpha/\xi)(|x_1| + |x_2|)kT$$

which is the "height" of the wall at $(x_1,x_2)$ above the $x_1$–$x_2$ plane. Sections through the origin parallel to the $x_1$ and $x_2$ axes reproduce the potentials $U(x_1)$ and $U(x_2)$ shown in Figures 9 and 8. The motion of the diffusing point in the $x_1$ direction (with diffusion coefficient $D_1$) and in the $x_2$ direction (with diffusion coefficient $D_2$) is independent, and a basic diffusion step as shown in Figure 7 is taken whenever the particle "escapes" the inside of the pyramid at its base edges, i.e., whenever

$$2|x_1| + |x_2| = N_b\xi \qquad \text{(AII.2)}$$

This implies the boundary condition $P(x_1,x_2,t) = 0$ on the base edges (AII.2).

The solution to (AII.1) subject to the boundary condition on $P(x_1,x_2,t)$ may be carried out numerically. Here we adopt a more physical approach. First, rewrite (AII.1) as

$$\partial P/\partial t = [\mathcal{L}_1(x_1) + \mathcal{L}_2(x_2)]P \qquad \text{(AII.3)}$$

with the operators

$$\mathcal{L}_i(x_i) = D_i\left[\frac{\partial^2}{\partial x_i{}^2} + \frac{2\alpha}{\xi}\frac{\partial}{\partial x_i}\right] \qquad i = 1, 2$$

(since $|\partial U/\partial x_1| = |\partial U/\partial x_2| = 2\alpha kT/\xi$).

Define

$$\tau(x_1,x_2) = \int_{t=0}^{\infty} P(x_1,x_2,t)\, dt$$

and operate $\int_0^\infty dt$ on both sides of (AIII.3).

This gives

$$P(x_1,x_2,\infty) - P(x_1,x_2,0) = [\mathcal{L}_1 + \mathcal{L}_2]\tau \qquad \text{(AII.4)}$$

Now $P(x_1,x_2,\infty) = 0$, and $P(x_1,x_2,0)\, dx_1\, dx_2$ is the equilibrium probability of finding the diffusing particle at $(x_1,x_1+dx_1)$, $(x_2,x_2+dx_2)$, given by a Boltzmann factor

$$P(x_1,x_2,0) = A_0 e^{-2\alpha|x_1|/\xi}e^{-2\alpha|x_2|/\xi}$$

where the normalizing constant is

$$A_0 = \left[\int_{x_1=-N_b\xi/2}^{N_b\xi/2}\int_{x_2=-N_b\xi}^{N_b\xi} P(x_1,x_2,0)\, dx_1\, dx_2\right]^{-1} = \frac{\alpha^2}{2\xi^2} \qquad \text{for } N_b \gg 1 \qquad \text{(AII.5)}$$

Equation AII.4 becomes

$$(\mathcal{L}_1 + \mathcal{L}_2)\tau + A_0 e^{(-2\alpha/\xi)(|x_1|+|x_2|)} = 0 \qquad \text{(AII.6)}$$

Since we assume the center monomer motion (varying $x_2$) and the arm-retraction mechanism (varying $x_1$) are independent modes, consider $\tau(x_1,x_2)$ for a *given* $x_1$ (written $\tau_{x_1}$). This corresponds to diffusion of our particle along the broken line in Figure 10, given by a section of the pyramid at $x_1$ parallel to the $x_2$ axis. Along this line the diffusion equation becomes

$$\mathcal{L}_2\tau_{x_1} + A' e^{(-2\alpha/\xi)|x_2|} = 0 \qquad \text{(AII.7)}$$

with the boundary condition $\tau_{x_1} = 0$ at $x_2 = \pm(N_b\xi - 2|x_1|)$ and $A' = A_0 e^{(-2\alpha/\xi)|x_1|}$. Equation AII.7 may be readily solved for $\tau_{x_1}$ (which corresponds physically to all diffusion modes with a fixed amount of arm folding and a center monomer

which moves up an arm tube); an overall expectation time for this mode may be obtained over the various mode configurations $x_1$

$$\langle \tau_{x_1} \rangle_{x_2} = \int_{x_1=-N_b\xi/2}^{N_b\xi/2} \left[ \int_{x_2=-(N_b\xi-2|x_1|)}^{x_2=(N_b\xi-2|x_1|)} \tau_{x_1} \, dx_2 \right] dx_1$$

with a leading term

$$\langle \tau_{x_1} \rangle_{x_2} = \frac{A_0 \xi^4}{12\alpha^4 D_2} e^{2\alpha N_b} \qquad \text{for } N_b \gg 1 \qquad \text{(AII.8)}$$

on solving eq AII.7 explicitly for $\tau_{x_1}$.

Similarly, we can fix $x_2$ and consider diffusion along the cut represented by the dotted line in Figure 10. This leads to a diffusion equation for $\tau_{x_2}$ similar to (AII.7), and an overall expectation time for all modes (where the center is fixed at different points $x_2$ up an arm tube and the rest of the arm retracts) obtained over the various configurations $x_2$

$$\langle \tau_{x_2} \rangle_{x_1} = \int_{x_2=-N_b\xi}^{N_b\xi} \left[ \int_{x_1=-(N_b\xi-|x_2|)/2}^{+(N_b\xi-|x_2|)/2} \tau_{x_2} \, dx_1 \right] dx_2$$

with a leading term

$$\langle \tau_{x_2} \rangle_{x_1} = \frac{1}{6} \frac{A_0 \xi^4}{\alpha^4 D_1} e^{\alpha N_b} \qquad \text{for } N_b \gg 1 \qquad \text{(AII.9)}$$

Because of the exponential, we have

$$\langle \tau_{x_1} \rangle_{x_2} \gg \langle \tau_{x_2} \rangle_{x_1} \qquad \text{for } N_b \gg 1 \qquad \text{(AII.10)}$$

The physical significance of this is that most diffusive steps (i.e., escape at the pyramid base edges) will take place at lower $x_2$ values (center motion up a tube) and correspondingly higher $x_1$ values, as we would also expect intuitively. To a good approximation then we take the expectation time for the general mode of Figure 7 as $\tau_s \simeq \langle \tau_{x_2} \rangle_{x_1}$. Substituting for $A_0$ and $D_1$ (eq AII.5 and AI.11), we find

$$\tau_s = \frac{\tau_{rep}(n_b)}{12\alpha^2 N_b^2} \exp(\alpha N_b) \qquad f = 3$$

as given by eq III.18 in the text.

## Appendix III

We wish to estimate the probability $P_R^L(N_R)$ that an $N_R$ step cyclic random walk on an obstacle lattice has a nonramified, non-obstacle-enclosing ("sausagelike") configuration as indicated in Figure 7c.

At the crudest level we may impose the requirement that after $N_R/2$ steps, the remaining $N_R/2$ steps must exactly retrace the initial steps (Figure 11). In a $x$-coordination lattice the total number of ways an $N_R$ walk can come back to itself is $Q_1 = P(0)z^{N_R}$, where $P(0) \simeq N_R^{-3/2}$ (eq III.21). The number of ways of taking the first $N_R/2$ steps is just $Q_2 = z^{N_R/2}$, and if we impose exact retracing by the remaining steps, there is just one way of doing this, so that the probability may be estimated as

$$P_R^L(N_R) \simeq Q_2/Q_1 \simeq (\text{const}) N_R^{3/2} z^{-N_R/2} \qquad \text{(AIII.1)}$$

(AIII.1) represents a lower bound on $P_R^L$, since in practice we may regard sausage structures as nonramified (for purposes of diffusion) even if they have "small" unentangled loops sticking out, as indicated in Figure 7c. However, (AIII.1) gives us a feel for the problem. Lattice expressions for the constant $\gamma$ appearing in eq III.3 for $P_1(N)$ have the form[22,24]

$$\gamma = \log [z/2(z-1)^{1/2}]$$

If we identify $\gamma$ with the value $\alpha \simeq 0.6$–$0.7$ obtained by fitting to viscoelastic data on star melts,[21,22,24] we find the plausible value $z \simeq 10$ as an effective "coordination number" in polymer melts. We then rewrite eq AIII.1

$$P_R^L = (\text{const}) N_R^{3/2} e^{-N_R \ln z^{1/2}} = (\text{const}) \exp\left[ -\left( \beta - \frac{3}{2N_R} \ln N_R \right) N_R \right] \qquad \text{(AIII.2)}$$

where $\beta \simeq 1.1$ for $z = 10$. The limit of this expression at large $N_R$ appears as eq III.24 in the text.

## References and Notes


(1) Edwards, S. F. *Proc. Phys. Soc.* **1967**, *92*, 9.
(2) de Gennes, P.-G. *J. Chem. Phys.* **1971**, *55*, 572.
(3) Doi, M.; Edwards, S. F. *J. Chem. Soc., Faraday Trans. 2* **1978**, *74*, 1789, 1802, 1818; **1979**, *75*, 38.
(4) Curtis, C. F.; Bird, R. B. *J. Chem. Phys.* **1981**, *74*, 2016, 2026.
(5) Graessley, W. W. *Adv. Polym. Sci.* **1982**, *47*, 67 and references therein.
(6) Ferry, J. D. "Viscoelastic Properties of Polymers"; 3rd ed.; Wiley: New York, 1980.
(7) Klein, J. *Nature (London)* **1978**, *274*, 143.
(8) Leger, L.; Hervet, H.; Rondelez, F. *Macromolecules* **1981**, *14*, 1732. Nemoto, N.; Landry, M. R.; Kitano, T.; Wesson, J. A.; Yu, H. *Macromolecules* **1985**, *18*, 308.
(9) Amis, E. J.; Han, C. C. *Polymer* **1982**, *23*, 1403. Antonietti, M.; Coutandin, J.; Grutter, R.; Sillescu, H. *Macromolecules* **1984**, *17*, 798.
(10) Kimmich, R.; Bacchus, R. *Colloid Polym. Sci.* **1982**, *260*, 911.
(11) Fleischer, G. *Polym. Bull. (Berlin)* **1983**, *9*, 152.
(12) Bartels, C. R.; Crist, B.; Graessley, W. W. *J. Polym. Sci., Lett.* **1983**, *21*, 495; *Macromolecules* **1984**, *17*, 2702.
(13) Mills, P. J.; Green, P. F.; Palmstrom, C. J.; Mayer, J. W.; Kramer, E. J. *Appl. Phys. Lett.* **1984**, *45*, 957.
(14) Green, P. F.; Mills, F. J.; Palmstrom, C. J.; Mayer, J. W.; Kramer, E. J. *Phys. Rev. Lett.* **1984**, *53*, 2145.
(15) Evans, K. E.; Edwards, S. F. *J. Chem. Soc., Faraday Trans. 2* **1981**, *77*, 1891. Baumgartner, A.; Kremer, K.; Binder, K. *Faraday Symp. Chem. Soc.* **1983**, *18*, 37.
(16) The experimental situation concerning self-diffusion of entangled polymers is comprehensively reviewed in a recent report by: Tirrell, M. *Rubber Chem. Technol.* **1984**, *57*, 523.
(17) Klein, J. *Macromolecules* **1978**, *11*, 852.
(18) Daoud, M.; de Gennes, P.-G. *J. Polym. Sci., Polym. Phys. Ed.* **1979**, *17*, 1971.
(19) Klein, J. *Philos. Mag. A* **1981**, *43*, 771.
(20) de Gennes, P.-G. *J. Phys. (Les Ulis, Fr.)* **1975**, *36*, 1199.
(21) Doi, M.; Kuzuu, N. Y. *J. Polym. Sci., Polym. Lett.* **1980**, *18*, 775.
(22) Pearson, D. S.; Helfand, E. *Faraday Symp. Chem. Soc.* **1983**, *18*, 189.
(23) Marrucci, G. In "Advances in Transport Processes"; Mujumdar, A. S., Mashelkar, R. A., Eds.; Wiley: New York, 1984; Vol. V.
(24) Needs, R. J.; Edwards, S. F. *Macromolecules* **1983**, *16*, 1492.
(25) Fetters, L. J. *Polym. Prepr. (Am. Chem. Soc., Div. Polym. Chem.)* **1982**, *23*, vii.
(26) Klein, J. *Polym. Prepr. (Am. Chem. Soc., Div. Polym. Chem.)* **1981**, *22*, 105.
(27) Klein, J.; Fletcher, D.; Fetters, L. J. *Faraday Symp. Chem. Soc.* **1983**, *18*, 159.
(28) See, for example, the papers in the recent Faraday Symposium on "Molecular Basis of Viscoelasticity" (*Faraday Symp. Chem. Soc.* **1983**, *18*).
(29) Graessley, W. W. *J. Polym. Sci., Polym. Phys. Ed.* **1980**, *18*, 27.
(30) Rouse, P. *J. Chem. Phys.* **1953**, *21*, 1213.
(31) Zimm, B. *J. Chem. Phys.* **1956**, *24*, 269.
(32) Freed, K. F.; Edwards, S. F. *J. Chem. Phys.* **1974**, *61*, 3626.
(33) Richter, D.; Binder, K.; Ewen, B.; Stuhn, B. *J. Chem. Phys.*, in press.
(34) Zimm, B. H.; Kilb, R. W. *J. Polym. Sci.* **1959**, *37*, 19.
(35) Bloomfield, V. A.; Zimm, B. H. *J. Chem. Phys.* **1966**, *44*, 315.
(36) Montfort, J.-P. These d'Etat, Universite de Pau et des Pays de l'Adour, 1984. Montfort, J.-P.; Marin, G.; Monge, Ph. *Macromolecules* **1984**, *17*, 1551.
(37) Rachapudy, H.; Smith, G. G.; Raju, V. R.; Graessley, W. W. *J. Polym. Sci., Polym. Phys. Ed.* **1979**, *17*, 1211.
(38) McKenna, G. B.; Hadziioannou, G.; Lutz, P.; Hild, G.; Strazielle, C.; Rempp, P.; Kovacs, A. J. presented at Mar 1984 meeting of Division of High Polymer Physics, American Physical Society.

(39) Mills, P. J.; Mayer, J. W.; Kramer, E. J.; Hadziioannou, G.; Lutz, P.; Strazielle, C.; Rempp, P.; Kovacs, A.—Abstract submitted for APS meeting, Baltimore, March 1985. Also Poster—Gordon Polymer Physics Conference, July 1984.
(40) For example, $\tau_c = (1/6)\tau_{rep}(p)$ in the calculation of ref 17.
(41) I am indebted to Prof. de Gennes for discussions concerning this approach.
(42) $A$ is of order $\alpha(f-2)$ for large $N$.
(43) Following submission of this paper we became aware of recent work by N. Hadjichristidis and J. Roovers (*Polymer*, in press) indicating that the viscosity of four-arm polybutadiene (PBD) stars is indeed some 25% higher than for three-arm PBD stars with identical arms, a trend that appears to support our prediction.
(44) J. Roovers has just published (*Macromolecules* **1985**, *18*, 1359) viscosity–molecular weight data for ring–polystyrene melts.

# Brownian Dynamics Simulation of Wormlike Chains. Fluorescence Depolarization and Depolarized Light Scattering

**Stuart A. Allison**

*Department of Chemistry, Georgia State University, Atlanta, Georgia 30303.*
*Received May 3, 1985*

ABSTRACT: Brownian dynamics is used to simulate fluorescence depolarization and depolarized light scattering from a discrete wormlike chain model. Flexible constraints are used to hold adjacent subunits at a nearly constant separation. "Experiments" with rigid and flexible constraints were essentially identical. Preaveraging hydrodynamic interaction was found to have a negligible effect on 10-subunit chains for the experiments carried out in this work. Simulations on 30-subunit chains were carried out with preaveraging. Fluorescence depolarization was observed to be more sensitive to internal motion than depolarized light scattering. The fluorescence depolarization was also found to be very sensitive to the persistence length. Excellent agreement between the Barkley–Zimm theory of bending (Barkley, M. D.; Zimm, B. H. *J. Chem. Phys.* **1979**, *70*, 2991) and the fluorescence depolarization simulations was also obtained.

## I. Introduction

Computer simulations of long-range motion in macromolecules have increased greatly in recent years. Because these motions are generally slow, techniques other than conventional molecular dynamics must be used to study them. Brownian dynamics simulation methods have proven to be particularly useful in this regard.[1-4] To cite a few applications, they have been used to study backbone motion and isomerization in simple chain molecules,[5-9] hinge bending[10] and helix–coil transitions[11] in proteins, ring-closure dynamics in alkane chains,[12] biomolecular diffusion-controlled reactions,[13,14] transport properties of rigid and flexible macromolecules,[15] and fluorescence depolarization from hinged macromolecules[16] as well as DNA restriction fragments.[17] Brownian dynamics is an appropriate method for highly damped systems and is the diffusional analogue of molecular dynamics. The simulation is carried out by numerical integration of the Langevin equation.[2-4] The solvent is represented by suitable frictional and random forces and possibly by modified potentials of mean force. A recent review by McCammon gives a clear physical picture of Brownian motion in the context of protein dynamics.[18]

The focus of this article is the bending and overall motions of wormlike chains. Wormlike chains are realistic models for stiff linear polymers like DNA. Analytic theories of Gaussian or Rouse–Zimm model chains, as pioneered by Kirkwood[19] and Zimm,[20] have been successful in interpreting long-time (low-frequency) experiments on high molecular weight polymers. These models are, however, inadequate when the short-time or high-frequency behavior is of interest. Dielectric dispersion, fluorescence depolarization, NMR, depolarized light scattering, and perhaps polarized dynamic light scattering at a large scattering vector are several experimental methods that probe rapid internal motions of polymers.

The fluorescence anisotropy decay of ethidium bromide bound to DNA is an illustrative example of rapid internal motion in stiff polymers.[21-24] Because the emission dipole of the dye is tilted by about 70° from the local helix axis, torsional rather than bending motions are primarily responsible for this depolarization. Nonetheless, the latter motions do contribute. Analytic theories by Barkley and Zimm,[25] and by Allison and Schurr,[26] as well as a recent analysis by Yoshizaki et al.,[27,28] accurately reproduce the nonexponential decay. Hence, the experiments appear to confirm the theories with regard to torsional motion. In addition to torsion, the theories of Barkley and Zimm[25] and Yoshizaki, Yamakawa, and co-workers[27,28] account for bending as well. Unfortunately, it has not been possible to study bending motions directly (in the absence of torsion) by fluorescence depolarization, since this would require the bound chromophore to have its emission dipole parallel to the local helix axis. An alternative is to carry out computer "experiments" on well-defined model systems.

In this work, the technique of Brownian dynamics is used to simulate fluorescence depolarization from a discrete wormlike chain model of DNA in which the emission dipole is in a parallel configuration. Depolarized light scattering is also illustrated. Chains made up of 10 or 30 subunits are used where the longer chains have a contour length of about 920 Å. For 10-subunit chains, simulations with preaveraged and without preaveraged hydrodynamic interaction are compared and shown to be in good agreement with each other. This is consistent with the results of Garcia de la Torre and co-workers.[29] All simulations on 30-subunit chains have preaveraged hydrodynamic interaction.

In the next section, we first present the discrete wormlike chain model. The Brownian dynamics algorithm is briefly described along with the treatments of hydrodynamic interaction that are used. A description of how one simulates a particular experiment concludes this section. In section III, we first examine the effects of varying the stretching force constant and preaveraged hydrodynamic

0024-9297/86/2219-0118$01.50/0 